

# Thermodynamic analysis of a novel solar water heating system during low sun radiation in Iran

## Author

Vahid Beygzadeh <sup>a\*</sup>  
Shahram Khalil Arya <sup>a</sup>  
Iraj Mirzaee <sup>a</sup>  
Gholamreza Miri <sup>b</sup>

<sup>a</sup>Department of Mechanical Engineering, Faculty of Engineering, Urmia University of Technology, Urmia, Iran

<sup>b</sup>Department of Business Management, National Iranian Oil Refining & Distribution Company, Tehran, Iran

## Article history:

Received : 18 March 2018  
Accepted : 9 June 2018

**Keywords:** Energy Efficiency; Exergy Efficiency; SLHPS; Solar Water Heating System; Pinch Point Temperature.

## ABSTRACT

*This paper reports a plenary thermodynamic model of a novel solar system for water heating in buildings. Energy and exergy analyses are used to characterize the exergy destruction rate in any component and calculate system overall efficiency. The system consists of a solar evaporator, a heat exchanger to produce hot water, and an auxiliary pump. A computer simulation program using EES software is developed to model the solar water heating system. The system provides hot water during the hours of low sun radiation. Thermodynamic analysis involves the designation of effects of heat exchanger pinch point and ambient temperatures on the energetic and exergetic performance of the solar water heating system. The performance parameters computed are exergy destruction, and energetic and exergetic efficiencies. The result showed that the main source of exergy destruction is the solar evaporator. In the solar evaporator, 92.85% of the input exergy was destroyed. The other main source of exergy destruction is the heat exchanger, at 4.15%. The overall energetic and exergetic efficiencies of the solar water heating system were approximately 60.17% and 3.002% respectively.*

## 1. Introduction

The increasing expense and rarity of oil, gas, and electricity has led to considerable attention on the necessity for a transition to renewable energy sources.

Solar energy will play an indispensable role in this endeavor, particularly for heating, cooling, and water heating in domestic and commercial buildings.

Recent interest in sustainability and green buildings has increased focus on solar energy devices for their nonpolluting and renewable qualities; replacing fossil fuel with domestic,

renewable energy sources can also enhance national security by reducing dependence on imported energy [1].

Solar water heating is now a major technology. Wide spread application of solar water heaters can decrease a considerable portion of conventional energy being used for heating water in buildings, factories, and other commercial and institutional organizations. Internationally, the market for solar water heaters has developed significantly during the last few decades.

Solar water heating is the conversion of sun energy into heat for water heating using a solar system. A diversity of configurations exist at varying costs to provide solutions in different climates and latitudes. Solar water heating

\* Corresponding author: Vahid Beygzadeh  
Department of Mechanical Engineering, Faculty of Engineering, Urmia University of Technology, Urmia, Iran  
Email: vbeygzadeh@gmail.com



**Nomenclature**

amb	ambient
AUX	auxiliary pump
$D_{ll}$	liquid line diameter
$D_o$	loop heat pipes outer diameter
$\delta_{PW}$ (m)	thickness of loop heat pipes primary wicks
E	Energy
$\dot{E}_{heat}$	exergy transfer by heat, kW
$F_R$	LHP heat removal factor
$G_b$	solar radiation, $W/m^2$
$\dot{j}$	exergy destruction rate (kW)
LHP	loop heat pipe
$L_{vh}$	vapor header length
$L_e$	solar evaporator length
$m_f$ (kg)	liquid filling mass
(Np)	number of wicks pores
PWM	number of meshes of primary wicks
$\dot{Q}_{FL}$ (kW)	filled liquid Mass limit
$\dot{Q}_{EL}$ (kW)	entrainment limit
$\dot{Q}_{VL}$ (kW)	viscous limit
SUN	Sun
SWM	number of meshes of secondary wicks
SOL, EVA	solar loop heat pipe evaporator
T	temperature $^{\circ}C$ or K
$T_{SUN}$	Sun temperature (K)
$U_l$	overall heat loss coefficient of the solar evaporator, $kW/m^2 K$
0	reference environment condition
$A_{SOL,EVA}$	solar loop heat pipe evaporator area (m <sup>2</sup> )
cv	control volume
$D_{vl}$	vapor line diameter
$\delta_w$ (m)	thickness of LHPs wicks
$\delta_{SW}$ (m)	thickness of LHPs secondary wicks
e	exit
$\dot{E}$	exergy rate, kW
f, i	fluid entering solar evaporator
h	specific enthalpy (kJ/kg)
i	inlet

$L_{ll}$	liquid line length
$L_{vl}$	vapor line length
$\dot{m}$	mass flow rate (kg/s)
$N_{LHP}$	number of loop heat pipes
P	pressure (kPa)
$\dot{Q}$	heat rate, kW
$\dot{Q}_{SL}$ (kW)	sonic limit
$\dot{Q}_{BL}$ (kW)	boiling limit
S	radiation absorbed by the solar loop heat pipe evaporator
s	specific entropy (kJ/kg-K)
SLHPS	solar loop heat pipe system
$\psi$	specific exergy
t	time
u	useful
$\dot{W}$	work rate, kW

**Greek symbols**

$\eta_{ex}$	exergy efficiency
$\psi$	specific exergy, kJ/kg
$\eta_{en}$	Energy efficiency
$\eta_{LHP}$	LHP optical efficiency

**2. Material and Methods**

In this section, the characteristics of the solar water heating system and its components are explained.

**2.1. System description**

Figure 2 indicates a solar water heating system containing a solar loop heat pipe system (SLHPS) and a plate heat exchanger to produce hot water.

This system uses solar energy in Tabriz in cold seasonal conditions (low sun radiation) to evaporate a working fluid (acetone in this study, with thermodynamic properties listed in Table 1) through the solar loop heat pipe evaporator, which drives a plate heat exchanger to produce hot water.

The solar loop heat pipe system is composed of the solar evaporator (which consists of 1044 wicked loop heat pipes), vapour and liquid lines, vapour and liquid

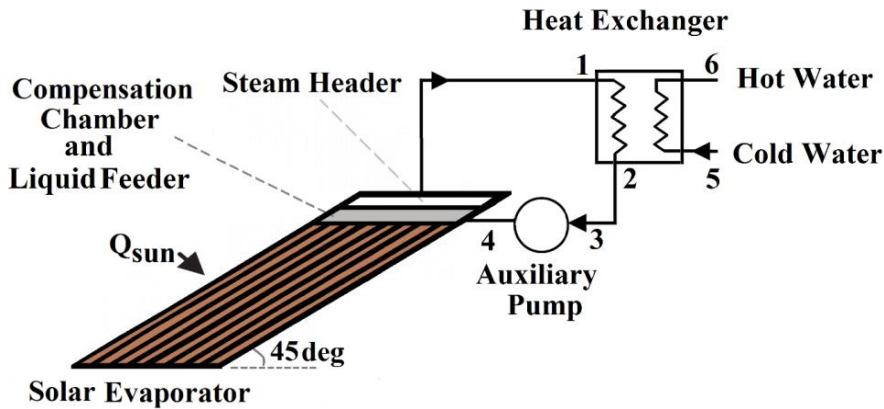


Fig. 2. Schematic of the proposed system

headers, compensation chamber, as well as a plate heat exchanger. The loop heat pipe evaporators are located on a copper plate in parallel lines with a small gap among them. In exploitation, the received solar energy transforms the acetone on the wicks of the loop heat pipes into vapour, which streams along the loop heat pipes to the vapour header due to the buoyancy of vapour; auxiliary pump pressure and gravity force created by the altitude discrepancy between the plate heat exchanger and the solar evaporator are illustrated at points 2 and 3 in Fig. 2. The vapour is then hauled to the plate heat exchanger through the vapour line.

Through the liquid line, the acetone liquid

enters the auxiliary pump. The auxiliary pump increases the pressure of SLHPS working fluid and the working fluid enters the compensation chamber placed under the vapour header. This amount of liquid is then divided to all loop heat pipes evaporators through a liquid feeder fixed at the over sector of the solar evaporator, as shown in Fig. 2. The liquid feeder would allow the liquid to descend into the solar evaporator. The schematic of LHP is shown in Fig. 3.

The loop heat pipe system uses a three path structure to supply rapid liquid distribution in the solar evaporator, as shown in Fig. 4.

The thermodynamic properties of the conventional heat pipes working fluids for low to moderate temperatures are listed in Table 2.

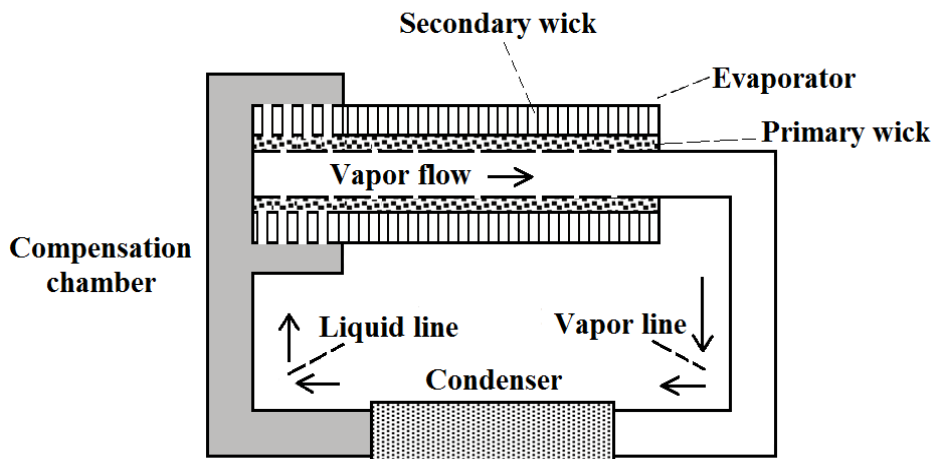


Fig. 3. The schematic of LHP

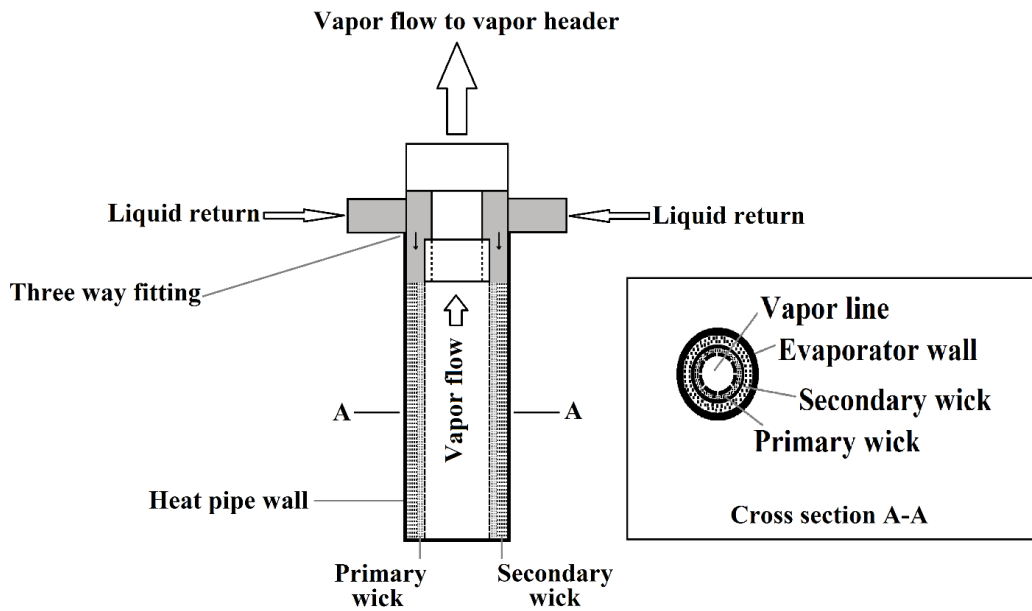


Fig. 4. Schematic of three way structure

Table 2. Thermodynamic properties of working fluids in conventional heat pipes

Working fluid	Critical pressure (MPa)	Critical temperature (°C)	Freezing temperature (°C)	Density (kg/m <sup>3</sup> )	Boiling temperature (°C)
N-pentane	3.364	196.5	-129.8	626	35.9 to 36.3
Neon	2.68	-228.7	-248.59	1207	-246.046
Oxygen	5.043	-118.6	-218.79	1141	-182.962
Nitrogen	3.396	-147	-210	808	-195.795
Ethane	4.872	32.17	-182.8	544.6	-88.5
Propane	4.247	96.68	-187.7	2.0098	-42.25 to -42.04
Propylene	4.665	92.42	-185.2	1.91	47.7
R152a	4.52	113.3	-117	900	-25
R11	4.408	198	-110.48	1494	23.77
Acetone	4.7	235	-94.7	784.5	56.05
Toluene	4.126	318.6	-95	870	111

Due to compatibility with the working conditions of SLHPS, acetone was selected as the working fluid in this study for the solar SLHPS system.

To carry out the thermodynamic analysis of the proposed system, these presumptions were used to make the analysis more tractable while retaining sufficient accuracy to illustrate the main points of the article:

- All the processes are considered to be operating at a steady state.
- Heat losses from piping and other components are insignificant.
- Thermal and radiation properties of the solar evaporator are considered independent of the temperature.
- All of the solar loop heat pipe system components are adiabatic, except loop heat pipes evaporators.
- Pressure drop in vapour and liquid headers was neglected.
- Pressure drops in vapour and liquid lines were neglected as they were rather small.
- Pressure drop in compensation chamber was neglected.
- The dead state is  $P_0 = 101kPa$  and  $T_0 = 298.15K$ .
- The ambient temperature is  $T_{amb} = 288.15K$ .

- The average solar radiation during low sun radiation was 200 W/m<sup>2</sup> (under Tabriz cold seasons conditions).
- The plate heat exchanger pinch point temperature was considered constant at 5°C .
- There was an axisymmetric stream in all the parts of the SLHPS.
- Chemical exergy of components and the kinetic and potential energy and exergy were neglected.

### 3. Analysis

For thermodynamic modeling, the proposed system (Fig. 2) was divided into two main parts: solar system and plate heat exchanger. The equations developed were programmed using Engineering Equation Solver (EES)

software. The input data used in this model is given in Table 3.

We specified the input and output enthalpy and exergy streams, exergy destructions rates, and energy and exergy efficiencies. The energy balances and governing equations for the main sections of the proposed system are described in the next subsections.

#### 3.1. Mass, energy and exergy analysis

Mass, energy and exergy balances for each control volume under steady state operation conditions with neglecting potential and kinetic energy changes can be expressed by:

$$\sum_k \dot{m}_i - \sum_k \dot{m}_e = \frac{dm_{cv}}{dt} \quad (1)$$

$$\frac{dE_{cv}}{dt} = \sum \dot{Q}_{cv} - \dot{W}_{cv} + \sum_i \dot{m}_i h_i - \sum_e \dot{m}_e h_e \quad (2)$$

**Table 3.** Input data for solar system

Solar evaporator length, (m)	3	Solar evaporator slope	45°
LHPs wicks length, (m)	3	Liquid filling mass, (kg)	2.2
Overall heat loss coefficient of the solar evaporator (kW/m <sup>2</sup> )	0.005	LHPs material	Copper
Solar evaporator heat removal factor	0.83	Solar evaporator optical efficiency	0.85
Solar evaporator to heat exchanger height difference	1	SLHPS condensers length, (m)	2
SLHPS heat exchanger height, (m)	2	LHPs mesh ratio (PWM/SWM)	2:1
Solar system operating temperature range	45-70°C	LHPs type	Mesh screen
Heat exchanger operating pressure range, (kPa)	0-4500	number of LHPs	1044
Heat exchangers plates thickness, (m)	0.002	Process heat exchanger (SLHPS condenser) hydraulic diameter, (m)	0.014
Heat exchanger (SLHPS condenser) hydraulic diameter, (m)	0.015	LHPs porosity	0.64
Thickness of LHPs wicks, (m)	0.0075	LHPs layers	Two layers
Thickness of LHPs secondary wicks, (m)	0.005	Effective diameter of wicks pores, (m)	0.1111
Thickness of LHPs primary wicks, (m)	0.0025	Number of wicks pores	9
Internal diameter of LHPs, (m)	0.049	SLHPS Vapour header material	Stainless steel
External diameter of LHPs evaporators, (m)	0.05	SLHPS vapour line material	Cast iron
Internal diameter of LHPs wicks vapour lines (m)	0.041	SLHPS liquid line material	Cast iron
Thermal conductivity of evaporator wall, (W/m.K)	394	LHPs walls thickness, (m)	0.001
Thermal conductivity of evaporator wick,(W/m.K)	394	SLHPS liquid line diameter, (m)	0.5
Heat exchangers conductivity, (W/m.K)	16	SLHPS liquid line length (m)	4
SLHPS vapour line diameter, (m)	0.6	SLHPS vapour line thickness, (m)	0.002
Solar evaporator pressure drop, (kPa)	11	SLHPS liquid line thickness, (m)	0.002
Heat exchanger (SLHPS condenser) pressure drop, (kPa)	6	SLHPS vapour line Length, (m)	3
LHPs evaporators length, (m)	3	Gravity effect pressure, (kPa)	+14.38

$$\frac{d\psi_{cv}}{dt} = \sum_i \dot{m}_i \psi_i - \sum_e \dot{m}_e \psi_e + \quad (3)$$

$$\sum_j (1 - \frac{T_0}{T_j}) \dot{Q}_j - (\dot{W}_{cv} - P_0 \frac{dV_{cv}}{dt}) - \dot{i}_{cv}$$

Where the net exergy transfer by heat ( $\dot{E}_{heat}$ ) at temperature T is given by:

$$\dot{E}_{heat} = \sum \dot{Q}_{cv} (1 - \frac{T_0}{T}) \quad (4)$$

And the specific exergy is given by:

$$\psi = (h - h_0) - T_0(s - s_0) \quad (5)$$

Then, the total exergy rate associated with a fluid stream becomes:

$$\dot{E} = \dot{m} \psi \quad (6)$$

The mass, energy and exergy balances and governing equations for the main sections of the solar water heating system shown in Fig. 2 are described in the next subsections.

### 3.2. Solar loop heat pipe system

In the solar loop heat pipe system with auxiliary pump, the system heat transfer capacity will be controlled by five limits (sonic, entrainment, viscous, boiling, and liquid filling mass limits) the minimum values of these limitations will be the actual retention of the solar loop heat pipe system heat transfer. The value of these limits are related to the thermal properties of the working fluids, loop heat pipes structure, and loop heat pipes working conditions.

According to Xingxing Zhang et al. [10], the heat transfer limits of the solar loop heat pipe system are shown in Table 4.

The thermodynamic analysis of the solar loop heat pipe system are presented in this subsection. To model the solar loop heat pipe system, we consider the approach used by John A. Duffie and William A. Beckman [11]. As shown in Fig. 2, acetone enters the solar loop heat pipe system (solar evaporator) at point 4 and is heated by the solar evaporator. The

useful heat gained by the working fluid can be written as:

$$\dot{Q}_u = \dot{m}_1 (h_1 - h_4) \quad (7)$$

where  $h_1, h_4$ , and  $\dot{m}_1$  are the acetone outlet enthalpy, inlet enthalpy, and mass flow rate.

The useful power produced by the solar loop heat pipe system is calculated as:

$$\dot{Q}_u = A_{SOL,EVA} F_R (S - U_l (T_4 - T_{amb})) \quad (8)$$

where  $T_{amb}$  is the ambient temperature and  $A_{SOL,EVA}$  is the solar loop heat pipe evaporator area, both of which can be expressed as:

$$A_{SOL,EVA} = N_{LHP} \pi D_o L_e \quad (9)$$

$F_R$  is the heat removal factor, which is around 0.83 for this case, and  $U_l$  is the overall solar evaporator loss coefficient.

In Eq. (8), radiation flux absorbed by the solar loop heat pipe evaporator is calculated as:

$$S = \eta_{LHP} G_b \quad (10)$$

where  $G_b$  is the solar radiation and  $\eta_{LHP}$  is the LHP optical efficiency.

The energy efficiency of the solar evaporator is expressed as:

$$\eta_{en,SOL,EVA} = \frac{\dot{Q}_u}{G_b A_{SOL,EVA}} \quad (11)$$

The exergy of a solar loop heat pipe evaporator is defined as:

$$\dot{E}_{SUN} = G_b A_{SOL,EVA} (1 - \frac{T_{amb}}{T_{SUN}}) \quad (12)$$

Where  $T_{SUN}$  is the sun temperature and equals to 4500 K.

The exergy destruction of the solar loop heat pipe evaporator is :

$$\dot{I}_{SOL,EVA} = \dot{E}_4 - \dot{E}_1 + \dot{E}_{SUN} \quad (13)$$

**Table 4.** The operating limits of the solar loop heat pipe system

<b>Entrainment limit</b> $\dot{Q}_{EL} (kW)$	<b>Viscous limit</b> $\dot{Q}_{VL} (kW)$	<b>Sonic limit</b> $\dot{Q}_{SL} (kW)$	<b>Boiling limit</b> $\dot{Q}_{BL} (kW)$	<b>Filled liquid Mass limit</b> $\dot{Q}_{FL} (kW)$
492.9768	8329	71026.45	165629.56	215.089

### 3.2.1. Validation of the solar evaporator model

The solar evaporator model was validated with an experimental study by E. Azad [12], as shown in Fig. 5. The model demonstrates good agreement with the experimental work.

### 3.3. Plate heat exchanger

Acetone vapour from the SLHPS enters the plate heat exchanger to produce hot water at about  $65^{\circ}\text{C}$ . Water enters this heat exchanger at a pressure and temperature of  $200\text{ kPa}$  and  $15^{\circ}\text{C}$  respectively. The energy and exergy balances for this component can be expressed, respectively, by:

$$\dot{m}_1(h_1 - h_2) = \dot{m}_5(h_6 - h_5) \quad (14)$$

$$\dot{I}_{HEX} = \dot{E}_5 + \dot{E}_1 - \dot{E}_2 - \dot{E}_6 \quad (15)$$

### 3.4. Overall analysis of the proposed system

The energy efficiency of the system is defined as:

$$\eta_{en} = \frac{\dot{Q}_{HEX} - \dot{W}_{AUX}}{G_b A_{SOL,EVA}} \quad (16)$$

The exergy efficiency of the system is defined as:

$$\eta_{ex} = \frac{\dot{E}_6 - \dot{E}_5 - \dot{W}_{AUX}}{\dot{E}_{SUN}} \quad (17)$$

Here,  $\dot{E}_{SUN}$  is the total inlet exergy to the system.

## 4. Results and Discussion

In this section, the results of thermodynamic modeling of the solar water heating system are presented. This section also assesses the effects of changing two of the design parameters on the system's performance.

### 4.1. Energy and exergy analysis results

The solar water heating system was analyzed using the above equations noting that the environment reference pressure and temperature are  $1.013\text{bar}$  and  $298.15\text{K}$  respectively. The thermodynamic properties of points for the solar water heating system at indicated nodes in Fig. 2 have been calculated using EES software and are summarized in Table 5.

The energy analysis results are summarized in Table 6. Energy analysis shows the energy transfer of each component of the proposed system and the energy efficiency of the solar water heating system.

The exergy analysis results are summarized in Table 7, and show that the highest exergy destruction rate happens in the solar evaporator, which is  $85.54\text{ kW}$ . The principal proof of this major exergy destruction rate is the large temperature discrepancy in the solar evaporator. Betterment potential is an index of possible improvement in the system from an exergetic point of view. As shown above, the

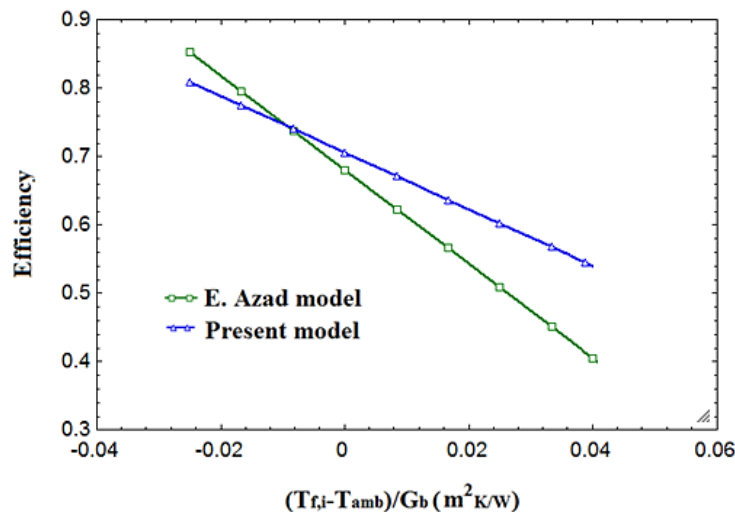


Fig. 5. Validation of the solar evaporator model as compared with E. Azad [12]



**Table 5.** The thermodynamic properties of points for the solar water heating system at indicated nodes in Fig. 2

State	Fluid	$\dot{m}$ (kg/s)	T(°C)	P(kPa)	h(kJ/kg)	S(kJ/kg.K)	$\dot{E}$ (kW)
1	Acetone	0.1	66.92	143.7	834.6	2.914	6.605
2	Acetone	0.1	20	137.7	242.3	1.149	0.01373
3	Acetone	0.1	20	152.1	242.3	1.149	0.01556
4	Acetone	0.1	20	154.7	242.3	1.149	0.01589
5	Water	0.28	15	200	63.11	0.2242	0.2287
6	Water	0.28	65.58	200	274.6	0.9005	2.995

**Table 6.** The results of energy analysis of the solar water heating system

Solar evaporator useful energy	59.23 kW
Heat exchanger energy flow	59.23 kW
auxiliary pump input power	0.0003896 kW
cycle efficiency	60.17 %

**Table 7.** The results of exergy analysis of the solar water heating system

Solar evaporator exergy destruction rate	85.54 kW
Heat exchanger exergy destruction rate	3.826 kW
Auxiliary pump exergy destruction rate	0.00005943 kW
cycle efficiency	3.002 %

major source of exergy destruction is the solar evaporator and, thus, it needs a precise design to improve its performance. An improved design contains, mainly, better optical efficiency of the loop heat pipes and lesser heat loss from the solar evaporator.

#### 4.2. Effect of varying heat exchanger pinch point temperature on solar water heating system performance

The heat exchanger pinch point temperature is a considerable design parameter in the proposed solar water heating system. Figure 6 shows the variation with plate heat exchanger pinch point temperature of the energy efficiency and exergy efficiency. As shown in this figure, increasing heat exchanger pinch point temperature reduces the heat flow of the plate heat exchanger. When the pinch point temperature increases, the heat absorbed by the

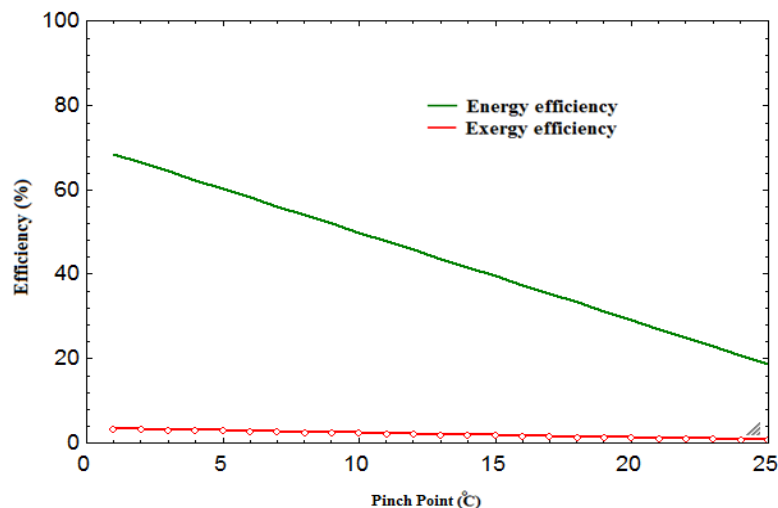


**Fig. 6.** Variation with heat exchanger pinch point temperature of the energy efficiency and exergy efficiency

plate heat exchanger decreases so that the utilization of this energy decreases: hence, the enthalpy of the hot water in the plate heat exchanger decreases, which reduces the heat flow and eventually leads to a decrease in the energy and exergy efficiencies of the solar water heating system.

#### 4.3. Effect of varying ambient temperature on solar water heating system performance

Another major parameter in the proposed system is ambient temperature because it affects the surface temperature and also the value for inlet exergy at each point of the solar water heating system. Hence, this temperature is a significant parameter. Figure 7 shows the variation of energy efficiency and exergy efficiency with ambient temperature. As can be seen, increasing the ambient temperature increases the energy and exergy efficiencies of the solar water heating system: due to an increase in the ambient temperature, the solar evaporator heat losses and exergy destruction rate decreases.

### 5. Conclusion

In this study, a steady state thermodynamic analysis of a solar driven water heating system was conducted in Tabriz under cold seasonal conditions.

The major aim of this study is the expansion and modeling of a new solar system with loop heat pipe solar evaporator for use in buildings.

Loop heat pipe has the potential to ease the difficulties in conventional solar thermal systems and is expected to be low cost and highly efficient.

The results of this thermodynamic analysis show that the main source of the exergy destruction is the solar evaporator. In the solar evaporator, 92.85% of the input exergy was annihilated. Another main source of exergy destruction is the heat exchanger, at 4.15%. The overall energetic and exergetic efficiencies of the solar water heating system were approximately 60.17% and 3.002% respectively.

SLHPS are capable of transference of a remarkable heat flux and can enhance the performance of solar water heating systems. SLHPS has some benefits as compared to the traditional heat pipe systems: for example, pliability in its layout and installation, which makes it proper for use in solar water heating systems.

Very few works has been done in the field of solar loop heat pipe systems and very opportunities exist for further development: for example, developing new, economically and energy and exergy efficient solar systems using loop heat pipes requires optimization of the structure of the solar system configuration to improve its energy and exergy. The results of this research are useful for understand the performance of the solar loop heat pipe evaporators so as to create new layouts related to the design of the solar loop heat pipe systems and promote solar thermal systems.

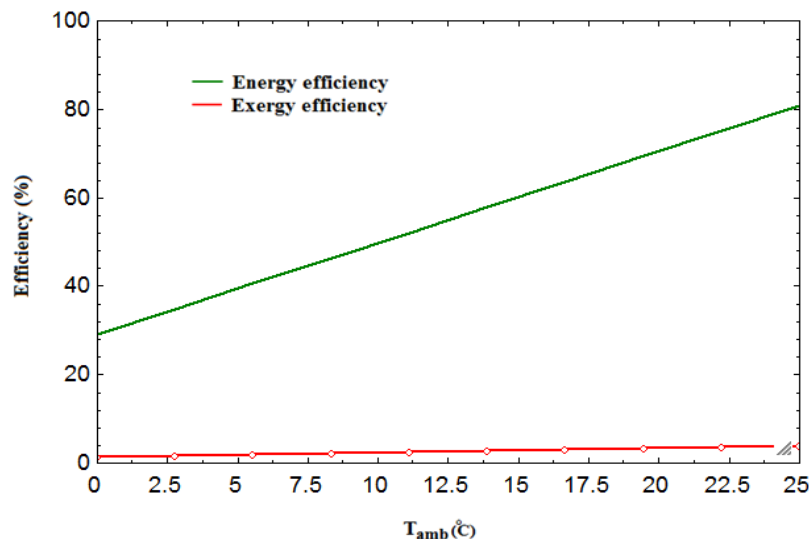


Fig. 7. Variation with ambient temperature of the energy efficiency and exergy efficiency

### Acknowledgements

The author is thankful to the management and staff of NIORDC for their technical support.

### References

- [1] McCartney W.J., 2011 Ashrae Handbook HVAC Applications (2011). McGraw-Hill.
- [2] Iran Renewable Energy and Energy Efficiency Organization Annual report (2010-2017).
- [3] Cengel Y. A., Heat Transfer a Practical Approach, 2th Edition (2003): 566. ISBN: 0072458933 9780072458930 0071151508 9780071151504, Boston: McGraw-Hill.
- [4] Sadiq M., Solar Water Heating System for Residential Consumers of Islamabad, Pakistan, A Cost Benefit Analysis, Journal of Cleaner Production (2018) 172: 2443-2453.
- [5] Mazarrón F.R., Porrás Prieto C. J., García J. L., Benavente R. M., Feasibility of Active Solar Water Heating Systems with Evacuated Tube Collector at Different Operational Water Temperatures, Energy Conversion and Management (2016) 113: 16–26.
- [6] Zainine M.A., Mezni T., Dakhlaoui M. A., Guizani A., Energetic Performance and Economic Analysis of a Solar Water Heating System for Different Flow Rates Values, A Case Study, Solar Energy (2017) 147: 164–180.
- [7] Allouhi A., Jamil a A., Kousksou T., Rhafiki T. E., Mourad Y., Zeraouli Y.. Solar Domestic Heating Water Systems in Morocco: An Energy Analysis, Energy Conversion and Management (2015) 92: 105–113.
- [8] Sathishkumar S., Balusamy T.. Performance Improvement in Solar Water Heating Systems, A Review, Renewable and Sustainable Energy Reviews (2014) 37: 191–198.
- [9] Wang Z., Yang W., A Review on Loop Heat Pipe for Use in Solar Water Heating, Energy and Buildings (2014) 79: 143–154.
- [10] Zhang X., Zhao X., Xu J., Yu X., Study of the Heat Transport Capacity of a Novel Gravitational Loop Heat Pipe, International Journal of Low-Carbon Technologies (2013) 8: 210–223.
- [11] Duffie J.A., Beckman W.A., Solar Engineering of Thermal Processes, 4th Edition (2013): 202-342 ISBN: 978-0-470-87366-3, New York: Wiley.
- [12] Azad E., Assessment of Three Types of Heat Pipe Solar Collectors, Renewable and Sustainable Energy Reviews (2012) 16: 2833–2838.